2-20-1997

Partitioning of the reactive nitrogen reservoir in the lower sratosphere of the southern hemisphere: Observations and modeling

R. S. Gao
National Oceanic and Atmospheric Administration

D. W. Fahey
National Oceanic and Atmospheric Administration

R. J. Salawitch
Jet Propulsion Laboratory

S. A. Lloyd
Johns Hopkins University

D. E. Anderson
Johns Hopkins University

See next page for additional authors

Recommended Citation

Gao, R. S., et al. (1997), Partitioning of the reactive nitrogen reservoir in the lower stratosphere of the southern hemisphere: Observations and modeling, J. Geophys. Res., 102(D3), 3935– 3949, doi:10.1029/96JD01967.

Authors

R. S. Gao, D. W. Fahey, R. J. Salawitch, S. A. Lloyd, D. E. Anderson, R. DeMajistre, C. T. McElroy, E. L. Woodbridge, R. C. Wamsley, S. G. Donnelly, L. A. Del Negro, M. H. Proffitt, R. M. Stimpfle, D. W. Kohn, S. R. Kawa, L. R. Lait, M. Loewenstein, J. R. Podolske, E. R. Keim, J. E. Dye, J. C. Wilson, and K. R. Chan

JOURNAL OF GEOPHYSICAL RESEARCH, VOL. 102, NO. D3, PAGES 3935-3949, FEBRUARY 20, 1997

Partitioning of the reactive nitrogen reservoir in the lower stratosphere of the southern hemisphere: Observations and modeling

R. S. Gao,[1,2] D. W. Fahey,[1] R. J. Salawitch,[3] S. A. Lloyd,[4] D. E. Anderson,[4] R. DeMajistre,[4] C. T. McElroy,[5] E. L. Woodbridge,[6] R. C. Wamsley,[1,2] S. G. Donnelly,[1,2] L. A. Del Negro,[1,2,7] M. H. Proffitt,[1,2] R. M. Stimpfle,[8] D. W. Kohn,[8] S. R. Kawa,[9] L. R. Lait,[9] M. Loewenstein,[10] J. R. Podolske,[10] E. R. Keim,[1,2] J. E. Dye,[11] J. C. Wilson,[12] and K. R. Chan[10]

Abstract. Measurements of nitric oxide (NO), nitrogen dioxide (NO_2), and total reactive nitrogen ($NO_y = NO + NO_2 + NO_3 + HNO_3 + ClONO_2 + 2N_2O_5 + ...$) were made during austral fall, winter, and spring 1994 as part of the NASA Airborne Southern Hemisphere Ozone Experiment/Measurements for Assessing the Effects of Stratospheric Aircraft mission. Comparisons between measured NO_2 values and those calculated using a steady state (SS) approximation are presented for flights at mid and high latitudes. The SS results agree with the measurements to within 8%, suggesting that the kinetic rate coefficients and calculated NO_2 photolysis rate used in the SS approximation are reasonably accurate for conditions in the lower stratosphere. However, NO_2 values observed in the Concorde exhaust plume were significantly less than SS values. Calculated NO_2 photolysis rates showed good agreement with values inferred from solar flux measurements, indicating a strong self-consistency in our understanding of UV radiation transmission in the lower stratosphere. Model comparisons using a full diurnal, photochemical steady state model also show good agreement with the NO and NO_2 measurements, suggesting that the reactions affecting the partitioning of the NO_y reservoir are well understood in the lower stratosphere.

Introduction

Stratospheric ozone (O_3) is destroyed in catalytic cycles involving oxides of hydrogen ($HO_x = OH + HO_2$), nitrogen ($NO_x = NO + NO_2$), chlorine ($ClO_x = Cl + ClO + 2ClOOCl$), and bromine ($BrO_x = Br + BrO$). Our understanding of O_3 destruction cycles changed significantly with the recognition of the role of heterogeneous reactions in the stratosphere [*Solomon et al.*, 1986; *McElroy et al.*, 1986, 1992; *Rodriguez et al.*, 1991; *Fahey et al.*, 1993; *Kolb et al.*, 1995; *Hanson et al.*, 1996]. On sulfate aerosol surfaces, the reactions

$$N_2O_5 + H_2O \xrightarrow{\text{aerosol}} 2HNO_3 \qquad (1)$$

$$ClONO_2 + H_2O \xrightarrow{\text{aerosol}} HOCl + HNO_3 \qquad (2)$$

$$BrONO_2 + H_2O \xrightarrow{\text{aerosol}} HOBr + HNO_3 \qquad (3)$$

reduce the concentrations of NO_x within the total reactive nitrogen ($NO_y = NO + NO_2 + NO_3 + HNO_3 + ClONO_2 + 2N_2O_5 + ...$) reservoir with nitric acid (HNO_3) product molecules released back into the gas phase. Since the abundance of NO_x also controls the partitioning between the hydroxyl radical (OH) and hydroperoxyl radical (HO_2) and between chlorine monoxide (ClO) and chlorine nitrate($ClONO_2$), these heterogeneous reactions strongly influence the O_3 destruction rate [*Cohen et al.*, 1994; *Stimpfle et al.*, 1994; *Wennberg et al.*, 1994]. With the resulting increase in HO_x and ClO_x concentrations, the net contribution to O_3 loss from the HO_x, ClO_x, and BrO_x catalytic cycles generally exceeds that of NO_x in the lower stratosphere. Midlatitude measurements of species in each radical family have confirmed this hierarchy in the catalytic cycles [*Salawitch et al.*, 1994a; *Wennberg et al.*, 1994]. Figure 1 illustrates the relation of reactions (1) through (3) to other photochemical reactions that affect the partitioning of NO_y

---

[1] Aeronomy Laboratory, National Oceanic and Atmospheric Administration, Boulder, Colorado.

[2] Cooperative Institute for Research in Environmental Science, University of Colorado, Boulder.

[3] Jet Propulsion Laboratory, Pasadena, California.

[4] Applied Physics Laboratory, Johns Hopkins University, Laurel, Maryland.

[5] Atmospheric Environment Service/Canada, Downsview, Ontario.

[6] Scripps Institution of Oceanography, University of California at San Diego, La Jolla.

[7] Department of Chemistry and Biochemistry, University of Colorado, Boulder.

[8] Department of Chemistry, Harvard University, Cambridge, Massachussetts.

[9] NASA Goddard Space Flight Center, Greenbelt, Maryland.

[10] NASA Ames Research Center, Moffett Field, California.

[11] Mesoscale and Microscale Meteorology Division, National Center for Atmospheric Research, Boulder, Colorado.

[12] Department of Engineering, University of Denver, Colorado.

Paper number 96JD01967.
0148-0227/97/96JD-01967$09.00

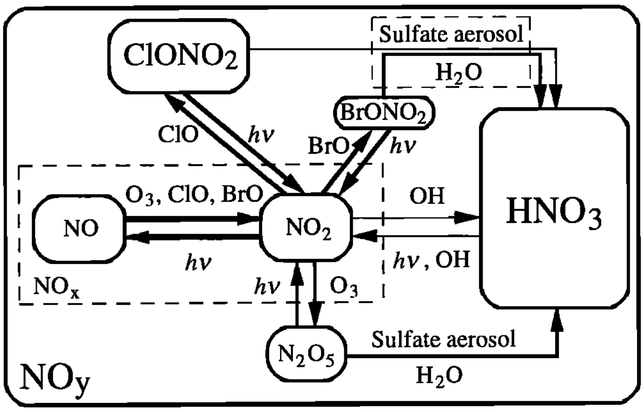

Figure 1. Diagram denoting the principal species of the NO_y reservoir and reaction pathways relevant to the lower stratosphere. Larger boxes and thicker arrows indicate a greater abundance and larger reaction rate, respectively. Photolysis is designated as *hv*.

species. Although it generally constitutes less than 10% of the NO_y reservoir, NO_x plays a pivotal role in establishing the abundance of the other NO_y component species.

Few stratospheric in situ measurements of nitrogen dioxide (NO_2) were made before 1994 [*Helten et al.*, 1984, 1985; *Hastie and Miller*, 1985; *McFarland et al.*, 1986; *Ridley et al.*, 1988; *Carroll et al.*, 1990; *Folkins et al.*, 1994], and not many of them include simultaneous measurements of NO_y. The most extensive in situ observations of reactive nitrogen made in the lower stratosphere include only measurements of nitric oxide (NO) and NO_y [*Fahey et al.*, 1993; *Kondo et at.*, 1992]. Our understanding of the partitioning of NO_y gases is facilitated by examining the NO_x/NO_y ratio, since the concentration of NO and NO_2 changes by large amounts during the day due primarily to changes in solar radiation, while the concentration of NO_x is nearly constant over a diurnal cycle. Past studies of the role of reactions (1) through (3) on NO_y partitioning, for example, have relied on estimating the NO_x/NO_y ratio using concentrations of NO_2 calculated from simultaneous measurements of NO, O_3, ClO, and theoretical values for the photolysis rate of NO_2, assuming steady state (SS) concentrations of NO and NO_2 [*Webster*, 1987; *Kawa et al.*, 1990, 1992]. Recent in situ measurements of NO_2 together with NO and NO_y made in the lower stratosphere during the 1993 NASA Stratospheric Photochemistry, Aerosol, and Dynamics Expedition (SPADE) provided an opportunity to test directly our understanding of the NO_x/NO_y ratio and the partitioning of NO and NO_2 [*Gao et al.*, 1994; *Jaeglé et al.*, 1994]. The concentrations of NO_2 from the Jet Propulsion Laboratory (JPL) Aircraft Laser IR Absorption Spectrometer (ALIAS) instrument and the National Oceanic and Atmospheric Administration (NOAA) Aeronomy Laboratory instrument used here were approximately 40% lower than SS abundances calculated with simultaneous measurements of NO, O_3, and ClO [*Jaeglé et al.*, 1994; *Salawitch et al.*, 1994b]. However, the uncertainties are ~20% and 60%, respectively, for the JPL and NOAA NO_2 measurements and ~60% for inferred NO_2 values. (The largest contribution to this uncertainty is from the reaction rate of NO + O_3). Consequently, the significance of the discrepancy between observation and theory for the NO/NO_2 ratio suggested by the SPADE observations remains unclear.

The NASA Airborne Southern Hemisphere Ozone Experiment/Measurements for Assessing the Effects of Stratospheric Aircraft (ASHOE/MAESA) mission was conducted in California, Hawaii, Fiji, and New Zealand from February to November 1994. Poleward flights (45°S to 68°S) by the NASA ER-2 high-altitude aircraft from Christchurch repeatedly reached the edge region of the Antarctic vortex throughout its lifetime. Simultaneous measurements of NO, NO_2, and NO_y are available from 10 ASHOE/MAESA flights, along with more than 20 other measurements of trace gases, radicals, aerosols, the solar radiation field, and meteorological parameters. Important improvements made to the NOAA Aeronomy Laboratory NO_2 detector between the SPADE and ASHOE/MAESA missions have reduced significantly the systematic errors in the NO_2 measurements. The combined ER-2 measurement set includes values of the photolysis rate of NO_2 (J_{NO_2}) from solar radiometer observations (on four flights), from an SS expression incorporating the trace gas observations (on all 10 flights) and from radiation scattering models. The calculation of SS NO_2 is performed using two of these independent J_{NO_2} values. Comparisons are presented for both modeled and measured values of J_{NO_2} and NO_2. The extensive ASHOE/MAESA data set also provides a unique opportunity to test our understanding of the partitioning within the NO_y reservoir over an extended time period in the lower stratosphere. Using 4 of the 10 flights, we present measured NO, NO_2 (three of four flights), and the NO_x/NO_y ratio from austral autumn to spring and compare these values to SS NO_2 values and the results from a photochemical stationary state model (PSS). Since no ALIAS NO_2 measurements were made during ASHOE/MAESA, comparisons similar to those made with SPADE data cannot be repeated here.

Measurements

The reactive nitrogen species NO, NO_2, and NO_y are measured with a three-channel chemiluminescence detector (CLD) on the ER-2 aircraft (Figure 2) [*Fahey et al.*, 1989, 1993; *Gao et al.*, 1994]. In the first CLD channel, NO is detected in an air sample using the chemiluminescence reaction with reagent O_3. The resultant excited-state NO_2 molecule subsequently relaxes to the ground state, emitting an infrared photon. A photomultiplier monitors the photons emitted by NO_2 molecules, providing a signal proportional to the ambient NO concentration. NO_y detection is achieved by using a gold catalytic converter upstream in the second CLD channel sample line. The catalytic converter reduces NO_y molecules to NO. For NO_2 detection a UV photolysis system located in the sample line of the third CLD channel is used to convert ~50% of NO_2 to NO with a sample residence time of 1 s. Measured NO is then the sum of ambient NO and NO produced from photolysis of ambient NO_2. The latter is determined by subtracting the ambient NO signal using values obtained simultaneously in the first channel.

When the NO_2 photolysis system was first operated during the SPADE mission [*Gao et al.*, 1994], uncertainties in the NO_2 measurements were dominated by the UV-induced artifact. This artifact occurs in the photolysis system when UV radiation used to photodissociate NO_2 releases NO or NO_2 from the wall of the cell in reactions involving other NO_y species. The most likely source of the earlier artifact is HNO_3 photolysis from short-wavelength (< 340 nm) UV radiation transmitted into

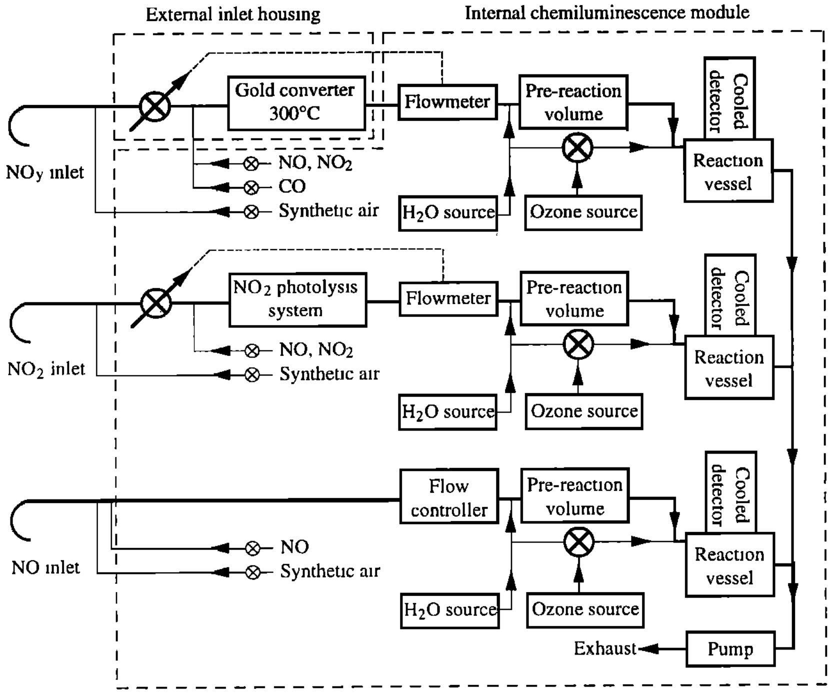

Figure 2a. Schematic of the NOAA Aeronomy Laboratory NO_y chemiluminescence detector. The internal chemiluminescence module resides inside the ER-2 fuselage (Figure 2b). The NO, NO_y, and NO_2 external inlets are located approximately 48, 48, and 25 cm below the fuselage, respectively. See *Fahey et al.* [1989] and *Gao et al.* [1994] for more detailed descriptions.

the photolysis cell, producing NO or NO_2. Since the HNO_3 concentration is at least an order of magnitude higher than that of NO_2 in the lower stratosphere, the photolysis of even a small fraction of HNO_3 can be a severe interference. During SPADE the NO_2 uncertainties of ~30 to 60% were primarily from the UV artifact. The largest sources of uncertainty in the present NO_2 measurements are (1) the UV artifact, (2) the subtraction of the ambient NO signal from the NO_2 channel response, and (3) the instrument background. However, in the current configuration the addition of a long-pass optical filter to the photolysis system has virtually eliminated the interference from HNO_3 as determined in laboratory tests. In flight the remaining UV artifact was checked periodically using the addition of synthetic air to the sample flow [*Gao et al.*, 1994]. Typical values of ~0.1 part per billion by volume (ppbv) were constant throughout a flight and comparable to those measured in the laboratory. Measurements of the artifact, photolytic conversion fraction of NO_2 to NO, and instrument background are obtained regularly throughout each flight and incorporated directly into the data reduction algorithm used to calculate the NO_2 mixing ratio.

The accurate subtraction of the ambient NO signal from the NO_2 channel signal relies on the assumption that NO is detected equivalently in both channels. As stated by *Gao et*

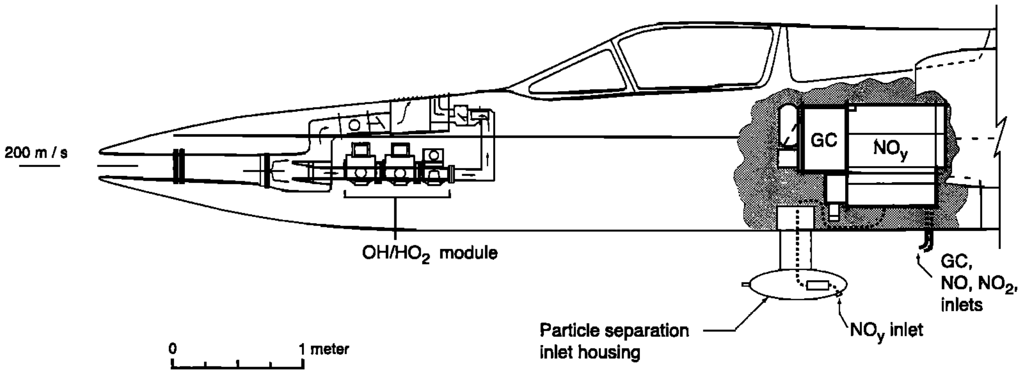

Figure 2b. Schematic of the forward fuselage of the ER-2 high-altitude aircraft showing the location of the reactive nitrogen (NO_y), gas chromatograph (GC) [*Elkins et al.*, 1996], and OH and HO_2 instruments [*Wennberg et al.*, 1995]. The NO_y inlet is shown at the rear of the external housing designed for particle separation. The NO_2 photolysis module is located in the lower forward section of the NO_y enclosure. The inlets for NO and NO_2 are mounted on the fuselage directly below the instrument. Addition of calibration gas to the sample lines occurs inside the fuselage for NO and NO_2 and inside the external housing upstream of the catalyst for NO_y.

al. [1994], in-flight checks during SPADE revealed that NO values from the NO channel were always 10% higher than from the NO_2 channel when the photolysis lamp was off. This difference persisted throughout the ASHOE/MAESA mission. Although the difference was corrected in the NO subtraction, a significant error is associated with this step. This error now represents the largest source of uncertainty in NO_2 measurements at midlatitudes where ambient NO concentrations typically exceed those of NO_2. Ambient NO_2 concentrations at high latitudes during polar winter are usually greater than those of NO, while NO_x concentrations are usually lower than at midlatitudes. At high latitudes the uncertainty associated with the instrument background predominates over other error sources. Overall, a systematic error estimate of ±20 to 30% applies when NO_2 mixing ratios are above 0.1 ppbv and NO_2/NO ratios are above unity and thus covers virtually all NO_2 data presented in this paper.

Another potential artifact source in the NO_2 measurement is the thermal decomposition of $ClONO_2$, N_2O_5, and HO_2NO_2 combined with the photolysis of decomposition products to form NO. Gas phase decomposition fractions depend on the temperature and residence time of the photolysis cell and inlet lines [*Gao et al.*, 1994]. For typical cell conditions (12°C and 1.1 s) associated with the data presented here, the respective gas phase decomposition fractions are all less than 1%. However, heterogeneous decomposition could further increase the artifact response. In-flight tests conducted to examine the effect of these decomposition processes in a system with higher cell temperatures and longer residence times were inconclusive [*Carroll et al.*, 1990]. The comparison of the ratio of measured to SS NO_2 values presented below is less than unity on average (0.92 ± 0.14) over a range of estimated $ClONO_2$, N_2O_5, and HO_2NO_2 values, thereby offering some evidence that NO_y interferences are not significant.

Solar irradiance between 300 and 775 nm was measured on the ER-2 with the Composition and Photodissociative Flux Measurement (CPFM) instrument [*McElroy*, 1995]. Using the wavelength-dependent flux data, the photodissociation rate of NO_2 as well as of other molecules can be derived [*McElroy et al.*, 1995]. Values of J_{NO_2} are typically in the range of 0.01 to 0.02 s^{-1} for solar zenith angles (SZA) less than 80°. In the ASHOE/MAESA data set, J_{NO_2} values from the CPFM instrument are available for the four flights where NO_2 measurements are also available. The uncertainties associated with the CPFM J_{NO_2} values of ~15% include the non-Lambertian cloud-scattering effect which leads to an overestimation of total scattered light.

The SS calculations and PSS model described below utilize the concentration of radicals and trace molecules, aerosol properties, and meteorological parameters measured by other instruments aboard the ER-2 during ASHOE/MAESA. Uncertainties associated with measured quantities are provided in Table 1.

SS Calculations

The basic reactions controlling the NO_2/NO ratio in the lower stratosphere are

$$NO + O_3 \rightarrow NO_2 + O_2 \qquad (4)$$

$$NO + ClO \rightarrow NO_2 + Cl \qquad (5)$$

$$NO + BrO \rightarrow NO_2 + Br \qquad (6)$$

$$NO_2 + h\nu \rightarrow NO + O \qquad (7)$$

Table 1. ER-2 Instrument Characteristics

Measurement	Accuracy, $\pm\sigma^a$	Sample Period, s	Reference
NO	15%	1	*Fahey et al.* [1989]
NO_2	20-30%	1	*Gao et al.* [1994]
NO_y	15%	1	*Fahey et al.* [1989]
O_3	5%	1	*Proffitt et al.* [1989b]
BrO	20%	3600	*Brune et al.* [1989a]
ClO	15%	16	*Brune et al.* [1989b]
J_{NO_2}	15%	164	*McElroy et al.* [1995]
Pressure	0.5 mbar	1	*Scott et al.* [1990]
Temperature	0.3K	1	*Scott et al.* [1990]
Aerosols	< 100%	10	*Jonsson et al.* [1995] *Baumgardner et al.* [1996]

^{a}Systematic error estimates.

where the reaction of HO_2 + NO can be ignored. The combined time constant of reactions (4) through (7) is of the order of 100 s in the lower stratosphere when the SZA is less than 85° [*DeMore et al.*, 1994]. Under this condition the assumption that NO and NO_2 are in photochemical steady state is valid; hence NO_2 can be expressed as

$$[NO_2] = \frac{[NO](k_{NO+O_3}[O_3] + k_{NO+ClO}[ClO] + k_{NO+BrO}[BrO])}{J_{NO_2}} \qquad (8)$$

where brackets indicate species concentrations and k values are rate coefficients [*DeMore et al.*, 1994]. The contribution of the BrO term, k_{NO+BrO}[NO][BrO], is sometimes neglected. In the ASHOE/MAESA data set, a compact correlation exists between the extensive measurements of BrO and CFC-11 (both at low time resolution, >> 1 s). Using the observed correlation, the data set of N_2O measurements at higher time resolution (1 s) and a similar compact correlation between N_2O and CFC-11, the bromine monoxide (BrO) mixing ratio is estimated for each 1-s point along the ER-2 flight track [*Woodbridge et al.*, 1995].

In addition to the J_{NO_2} values derived from the solar irradiance measurements, two sets of theoretical J_{NO_2} values were calculated independently for the ER-2 flight track. Both were calculated with isotropic, spherical, multiple-scattering models of the atmospheric radiation field and incorporate wavelength-dependent photolysis cross sections for NO_2 [*Prather*, 1981; *Anderson et al.*, 1995]. Both models used values of UV reflectivity (a surrogate for albedo) and total O_3 from the Total Ozone Mapping Spectrometer (TOMS) to calculate specific J values along the flight track. The wavelength-dependent transmission calculated by both models has been compared extensively as part of the 1995 Scientific Assessment of the Atmospheric Effects of Stratospheric Aircraft photolysis benchmark [*Stolarski et al.*, 1995]. Values from the two calculations show excellent agreement. For simplicity, only one set (based on *Prather* [1981] and used by *Salawitch et al.* [1994a, b]) is used in the SS and PSS model calculations and J_{NO_2} comparisons in this work. The uncertainty associated with modeling J_{NO_2} is estimated to be 30% based on comparable uncertainties for the radiative flux and NO_2 absorption cross section [*Jaeglé et al.*, 1994].

PSS Model Calculations

The PSS model is used in this work to calculate the steady state abundances of a variety of reactive species at ~15-min intervals throughout a 24-hour period by balancing the production and loss of each species integrated over a diurnal cycle [*Salawitch et al.*, 1994a, b]. Since the steady state solution includes the explicit diurnal variation of each species, detailed comparisons can be made to in situ observations along the ER-2 flight track by selecting model results for the corresponding local time. The PSS calculations use pressure, temperature, and latitude of air parcels encountered by the ER-2; measured concentrations of NO_y, O_3, water (H_2O), methane (CH_4), and aerosol surface area; and concentrations of inorganic chlorine (Cl_y) and inorganic bromine (Br_y) inferred from observed relations between chlorofluorocarbons [*Woodbridge et al.*, 1995] and brominated source gases [*Salawitch et al.*, 1994a; *Schauffler et al.*, 1993], respectively. Aerosol surface area values were obtained from the Focused Cavity Aerosol Spectrometer (FCAS), which detects the number concentration of particles with diameters between 0.06 and 2 μm [*Jonsson et al.*, 1995], and from the Multiple-Angle Aerosol Spectrometer Probe (MASP), which observes particles with diameters between 0.2 and 20 μm [*Baumgardner et al.*, 1996]. With the decay of aerosol loading since the Mount Pinatubo eruption in 1991, these diameter ranges include essentially all of the surface area of the background aerosol distribution.

The PSS model includes 35 reactive species and ~220 chemical reactions, with most reaction rates and absorption cross sections adopted from *DeMore et al.* [1994]. A reaction probability of 0.1 was used for the heterogeneous hydrolysis of N_2O_5 (R1). A reaction probability of 0.5 was used for the heterogeneous reaction of $BrONO_2 + H_2O$ (R3), based on recent laboratory measurements by *Hanson and Ravishankara* [1995]. The formulation of *Hanson and Ravishankara* [1994] and *Hanson et al.* [1994] were used for the rates of the heterogeneous reaction set $ClONO_2 + H_2O$ (R2) and $ClONO_2 + HCl$, and the heterogeneous reaction of hypochlorous acid (HOCl) and hydrogen chloride (HCl), respectively. Heterogeneous reactions involving HCl have a negligible effect on model results for temperatures encountered on these flights, except for certain poleward regions on the flight of August 6, 1994, as discussed below. The *Michelsen et al.* [1994] model, which allows for the photolysis of vibrationally and rotationally excited O_3, was used to calculate the quantum yields of the first excited state of atomic oxygen ($O(^1D)$) from O_3 photolysis. Finally, absorption cross sections for hydrogen peroxide (H_2O_2), nitrous acid (HONO), and peroxynitric acid (HNO_4) were extrapolated to longer wavelengths than in the work of *DeMore et al.* [1994] for a more accurate accounting of the photolysis of these gases at high SZA.

A Newton-Raphson iterative technique was used to find the set of diurnally varying species concentrations that repeats every 24 hours, thereby satisfying the criterion that production and loss for each species, integrated over a diurnal cycle, are equal [*Logan et al.*, 1978]. The photochemical lifetimes (mean concentrations divided by the integrated production rate) are <<1 day for HO_x, ~1 week for NO_x, and ~1 month for HCl. If before sampling by the ER-2, an air parcel has undergone excursions in either temperature or latitude that exceeds 10 K or 15°, respectively, then the PSS calculations may not be valid [*Kawa et al.*, 1993]. NO_x concentrations are especially sensitive to temperature and latitude history; OH is much less sensitive. A comparison of temperature and latitude of air parcels sampled by the ER-2 with the 10-day history of temperature and latitude, calculated using a trajectory model, is important for understanding where the PSS model may not be expected to provide a good simulation of NO_x.

Results and Discussion

NO and NO_2

The average volume mixing ratios of measured NO and NO_2 for each of the 10 flights are listed in Table 2. Results for

Table 2. Comparison of NO_2 Mixing Ratios Between Measurements and Steady State Calculations

				Measurements		NO_2 Steady State Calculation[a]			
Flight[b]	Latitude Coverage	SZA, deg	Data,[c] hours	NO, ppbv	NO_2, ppbv	Using Measured J_{NO_2}, ppbv[d]	Measured/ Calculated[e]	Using Calculated J_{NO_2}, ppbv[f]	Measured/ Calculated[e]
940214	37.5°N - 40.2°N	50° - 54°	0.7	0.17	0.19	0.21	0.90±0.10	0.20	0.93±0.16
940218	38.0°N - 60.8°N	62° - 73°	3.5	0.09	0.17	0.20	0.86±0.20	0.20	0.87±0.23
940318	22.9°N - 36.7°N	24° - 46°	2.0	0.40	0.30	0.30	0.99±0.07	0.34	0.91±0.07
940330	46.5°S - 66.6°S	55° - 80°	3.0	0.18	0.19	0.19	0.98±0.07	0.21	0.92±0.16
Average (4 flights)							**0.94±0.14**		**0.90±0.10**
940601	45.3°S - 60.9°S	70° - 85°	1.4	0.08	0.12			0.12	1.0±0.21
941008	40.1°S - 42.5°S	43° - 65°	1.0	0.15	0.14			0.16	0.91±0.14
941010	45.1°S - 70.0°S	51° - 67°	4.3	0.20	0.35			0.38	0.92±0.11
941013	43.8°S - 68.3°S	47° - 70°	4.4	0.19	0.34			0.38	0.91±0.09
941016	45.0°S - 69.5°S	45° - 58°	4.3	0.18	0.41			0.41	0.99±0.11
941020	46.5°S - 64.0°S	52° - 65°	3.1	0.29	0.37			0.41	0.90±0.09
Average (10 flights)									**0.92±0.14**

[a] Equation (8) is used for the steady state calculation.

[b] Read 940214 as February 14, 1994.

[c] Total combined length of data record used in flight.

[d] J_{NO_2} derived from measurements made by the Composition and Photodissociative Flux Measurement instrument.

[e] Average is calculated as $\left(\sum_n \frac{\text{measured } NO_2}{\text{calculated } NO_2}\right) / n$ where n is the number of 100-s averaged data points. Averages are shown with ±1σ standard deviation.

[f] J_{NO_2} calculated by *Salawitch et al.* [1994a, b].

individual flights are shown in Figures 3 and 4, with related measurements displayed in Figures 5 and 6. Average NO values are generally 0.2 ppbv or lower, with comparable or higher NO_2 values. SS NO_2 values from equation (8) were derived using theoretically calculated J_{NO_2} values and those from the solar radiation measurements. Measurements and calculations corresponding to SZA > 85° are excluded from Table 2. Measurements made in the Concorde plume on October 8, 1994, discussed in more detail below, also are excluded. Although no other data filtering is applied, most of the values correspond to pressures between 50 and 100 mbar (ER-2 cruise altitudes) in the lower stratosphere. The ratio of measured NO_2 to SS NO_2 values is averaged for individual as well as for all 10 flights. As shown in Table 2, good agreement exists between the measurements and the calculations, with no evidence of a seasonal or latitudinal dependence. The average measured NO_2 value is lower than the calculated SS values (equation (8)) by 8% . Excluding the NO + BrO reaction (not shown in Table 2) decreases the discrepancy to 5%. Thus the NO + BrO reaction, as the least important of the three loss processes for NO in equation (8), usually can be neglected in the lower stratosphere. Using solar J_{NO_2} values to calculate SS NO_2 appears to produce slightly better agreement than theoretical J_{NO_2} values, but the difference is much less than the uncertainties in both measurements and calculations.

The differences between measured and SS NO_2 values are significantly smaller than those found using the SPADE observations and less than the current experimental uncertainties (Table 1). The number of observations and the seasonal and latitudinal range of the data greatly exceed that of the SPADE data set. The primary NO_2 observations made during SPADE were obtained by the ALIAS instrument, which utilizes tunable diode laser absorption spectroscopy [*Jaeglé et al.*, 1994]. Using the SPADE comparison, SS NO_2 values have been reduced by a factor of 0.7 in other interpretive studies [*Wennberg et al.*, 1994]. On the basis of the ASHOE/MAESA results presented here, we do not recommend adjusting SS NO_2 values either by increasing J_{NO_2} values (as calculated from the radiation scattering models used here) or by reducing the NO + O_3 (R4) reaction rate constant, both of which are required to calculate the NO_2/NO ratio in the lower stratosphere.

Concorde Observations

On October 8, 1994, the ER-2 instruments sampled the exhaust plume of a Concorde supersonic passenger aircraft *in the lower stratosphere [Fahey et al.*, 1995a]. NO_x observations in several plume encounter events showed values to be well above background values. In the plume, NO and NO_2 reach steady state (equation (8)) within a few minutes with near-ambient concentrations of O_3, whereas the age of the exhaust at the time of sampling ranged from 10 to 60 min. For an age of 16 min, Figure 7 shows the comparison of measured and SS NO_2 values, where the expected good agreement was found outside the plume (Table 2). Inside the plume, however, peak values calculated for NO_2 are a factor of 2 higher than measured values. Furthermore, the sum of NO and SS NO_2 integrated inside the plume is ~10% higher than measured NO_y. Similar results were found as the plume age increased. Although instrumental issues cannot be completely ruled out, the most likely source of the discrepancy is that the SS expression (equation (8)) must be modified to account for other important reactions in the plume. For example, constituent species present only in the plume may react with NO_2 to form NO. The reaction may occur in the gas phase or may be a heterogeneous process involving the large number of aerosol particles observed in the plume [*Fahey et al.*, 1995a]. Alternatively, an increased abundance of aerosols in the plume may cause an increase in the effective value of J_{NO_2}. However, the J_{NO_2} enhancement needed to account for the data is larger than could be reasonably expected, based on calculations using a scattering model that describes the effect of aerosols on the radiation field. The consistency of the O_3-N_2O correlation through the plume encounters and the high dilution of the plume (10^5) indicates that O_3 values are free of artifacts in the plume and are essentially equal to ambient values. In an earlier study of the ER-2 plume [*Fahey et al.*, 1995b], measurements were obtained at night when NO is absent and no subtraction of the ambient NO signal is required to obtain an NO_2 value. In this case, the NO_x/NO_y ratio was 0.80, similar to values found in other plumes sampled during daylight. Thus NO_2 loss during sampling or other instrumental issues are unlikely to account for all of the discrepancy in the Concorde observations. At this point, the present data set is not sufficient to resolve this issue.

J_{NO_2} Values

The steady state value of J_{NO_2} can be expressed by rearranging equation (8) to yield

$$J_{NO_2} = \frac{[NO](k_{NO+O_3}[O_3] + k_{NO+ClO}[ClO] + k_{NO+BrO}[BrO])}{[NO_2]} \qquad (9)$$

Equation (9) allows J_{NO_2} values that are self-consistent with reactive trace species observations (chemical) to be compared with J_{NO_2} values inferred from the CPFM flux measurements (solar) or values calculated from a radiation transfer model (theoretical). The total measurement uncertainty in these chemically derived J_{NO_2} values (Figure 8) is estimated by propagating errors in the associated measurements (Table 1), assuming that there is no correlation of errors between individual measurements [*Bevington*, 1969]. Results shown in Figure 8 for the flight on March 18, 1994, show that the agreement between values of J_{NO_2} from the three methods is well within the measurement uncertainties at midlatitudes.

The chemical and solar values of J_{NO_2} derived from ER-2 measurements show more variability than the radiative-transfer model values. The model calculations rely on the TOMS satellite for both total column O_3 along the flight path and, more importantly, the effective UV reflectivity at a climatologically derived cloud height. Since the effective nadir footprint in the TOMS satellite data set is ~150 km, variability of the radiation field on small spatial scales is not resolved. Hence a model incorporating these data will not represent the subgrid scale variability of the real atmosphere. Work is currently in progress to correlate the abundance of species with a short photolytic lifetime (specifically OH and NO) with the variability of the radiation field observed by the CPFM instrument.

NOy partitioning

During ASHOE/MAESA, four ER-2 deployments were based in Christchurch, New Zealand, between March and October 1994. In each deployment, three or four ER-2 flights were made poleward of Christchurch reaching 65°-68°S latitude.

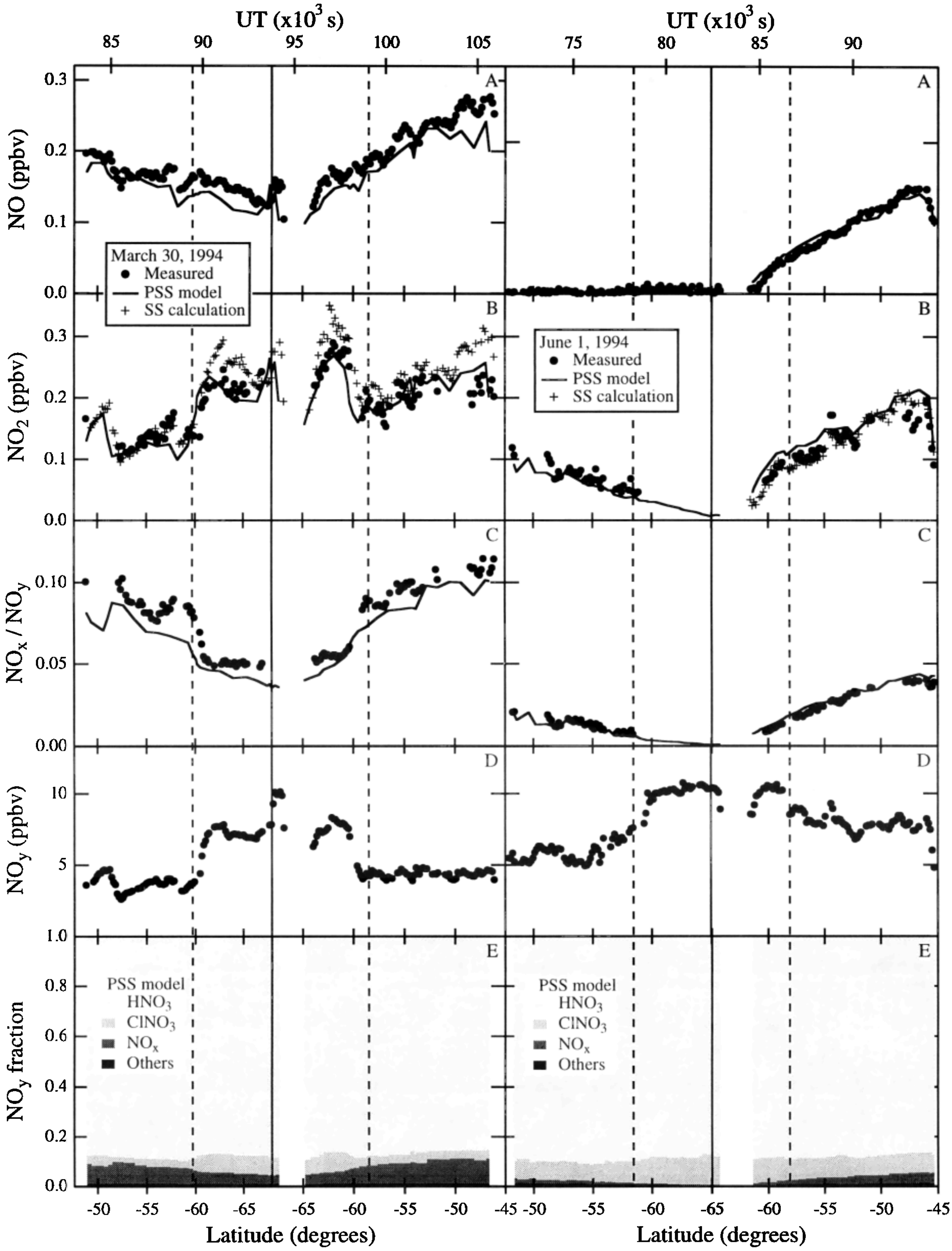

Figure 3. NO, NO_2, NO_x/NO_y, and NO_y mixing ratios measured on March 30 and June 1, 1994, are shown in panels A, B, C, and D, respectively (solid circles). The top axis represents universal time (UT) along the flight track and the bottom axis represents the approximate latitude in the southern hemisphere. Values for NO_2 from the steady state (SS) approximation (equation (8)) are shown in panel B (open diamonds). Measured and SS values are averaged over 100 s along the flight track (20 km). The photochemical steady state (PSS) model results are shown in panels A - D (solid lines) and in panel E. A pressure filter of 53-73 mbar (altitude range of 18.2-20.2 km) is applied to all results presented here. The vertical solid line in the middle of flight panel indicates the southernmost point of the flight track from Christchurch. The two dashed lines represent a reference point for the edge of the Antarctic vortex.

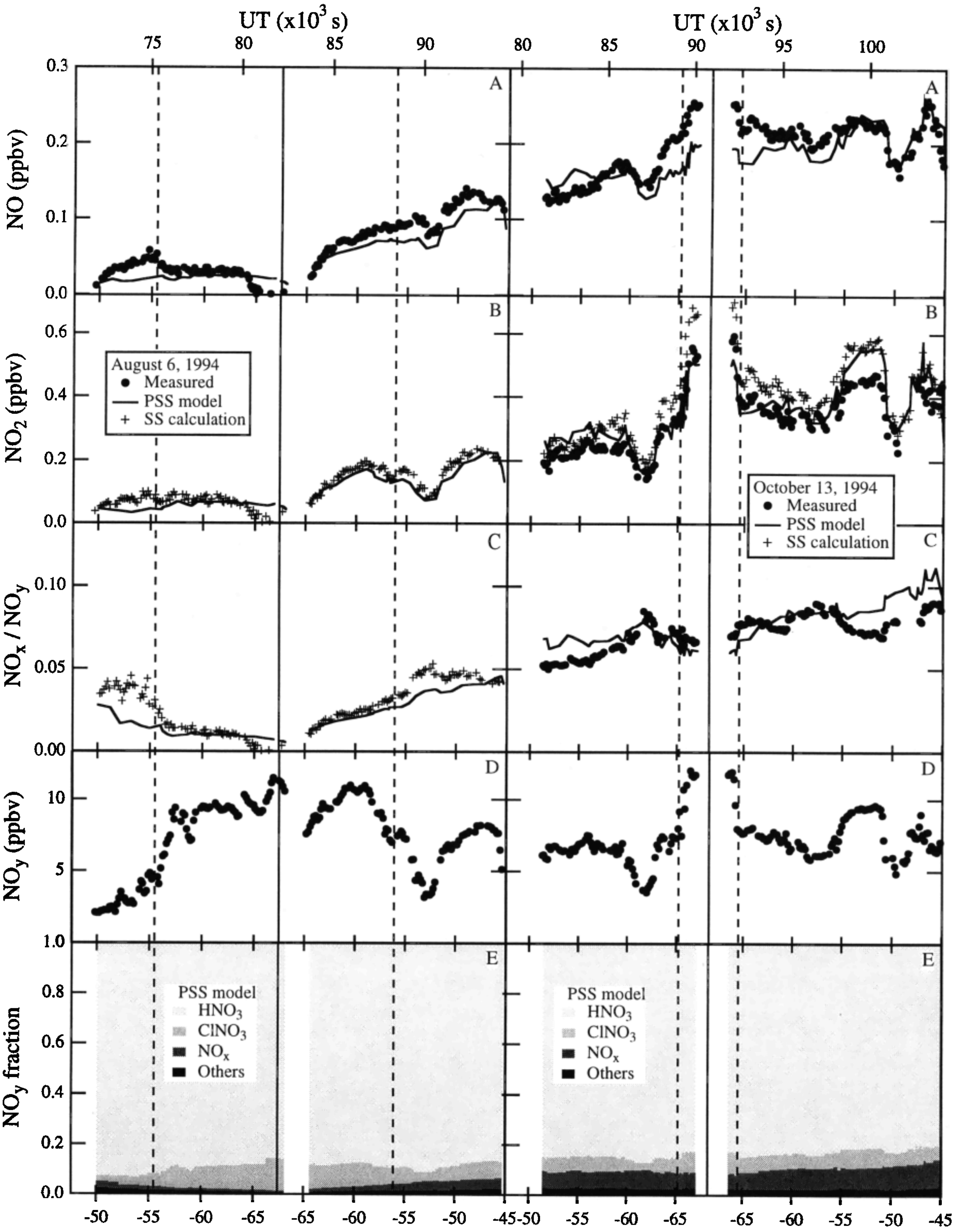

Figure 4. Measurements and model results for the flights of August 6 and October 13, 1994. Other details are the same as for Figure 3.

The flights were clustered in periods of about two weeks. Four flights (March 30, June 1, August 6, and October 13), one from each deployment, were chosen for a detailed evaluation of the partitioning within the NO$_y$ reservoir. The flights of March 30 and June 1 were chosen because of the availability of NO$_2$ measurements (compare Table 2). No NO$_2$ measurements are available for the late winter (July-August) deployment. However, the flight of August 6 was chosen because of interesting features in the measurements of other species, as discussed below. Since NO$_2$ measurements are available for all

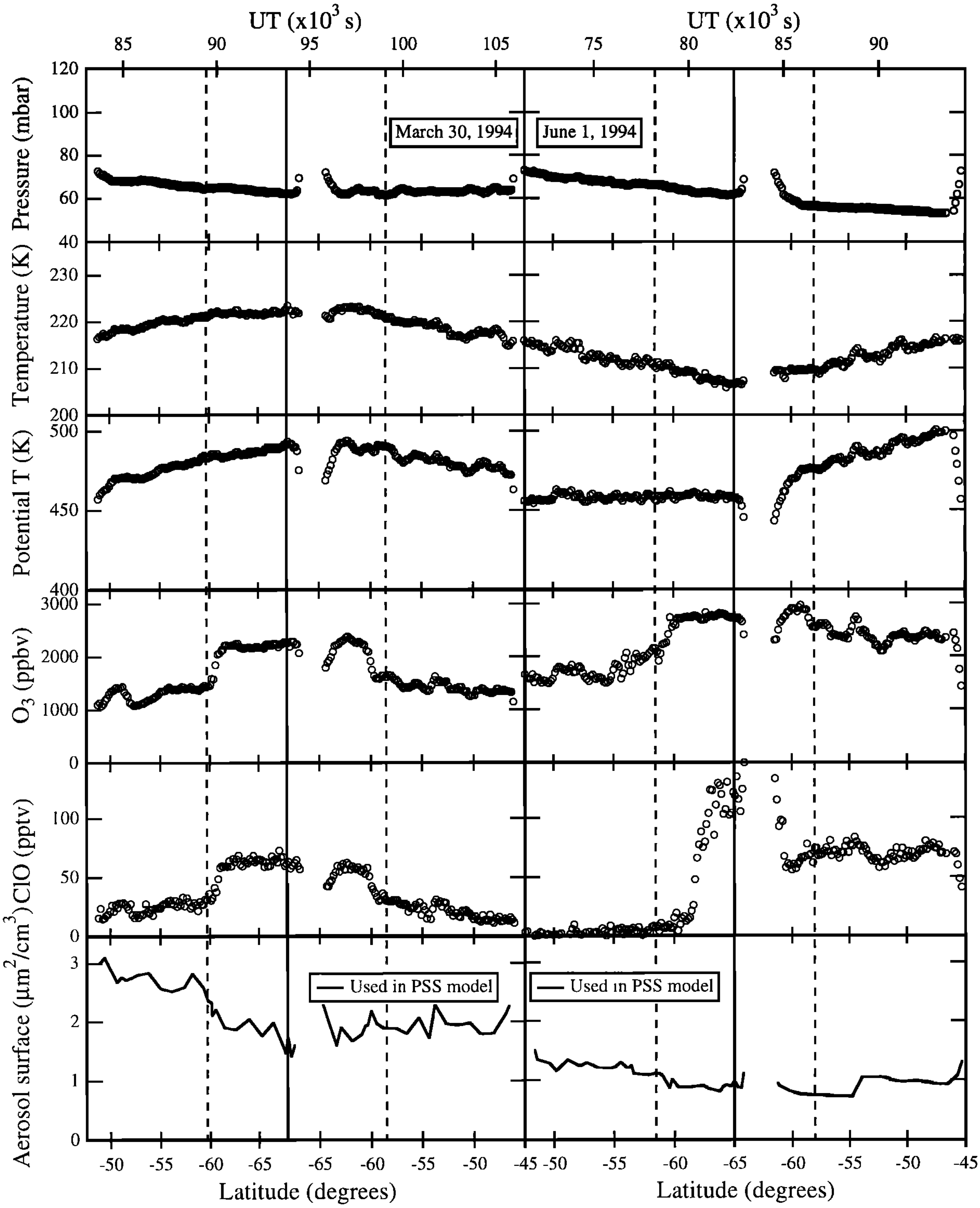

Figure 5. Related parameters and measurements made by other ER-2 instruments on March 30 and June 1, 1994, and used in the PSS model calculations. Aerosol values are estimated using the correlation with N_2O obtained on other flights in the March and June time periods.

poleward flights in October, one flight (October 13) was chosen to be representative. For each flight, measured values of NO, NO_2, NO_y, and NO_x/NO_y are plotted as a function of latitude in Figures 3 and 4. Also shown are NO_2 values from the SS approximation, using theoretically calculated J_{NO_2}, and NO and NO_2 values from the PSS model calculations. Finally, the PSS results for the fraction of NO_y attributed to HNO_3, $ClONO_2$, and NO_x are shown as a histogram. Data are shown only for ER-2 cruise conditions in the lower stratosphere (pressures between 53 and 73 mbar). The solid line in the middle of each figure indicates the poleward limit of each flight. A dashed line indicates a reference location in the

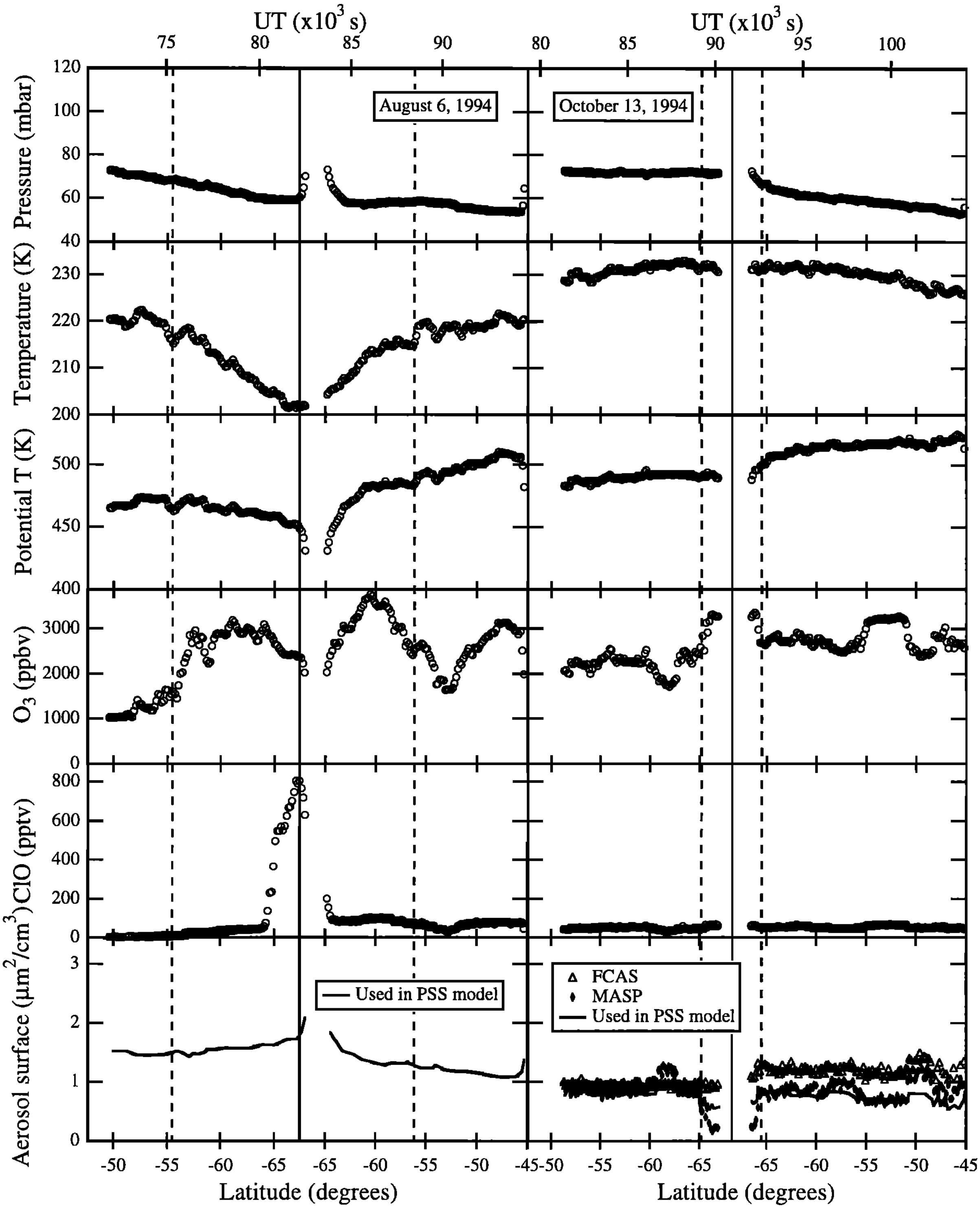

Figure 6. Related parameters and measurements made by other ER-2 instruments on August 6 and October 13, 1994, and used in the PSS model calculations. Aerosol surface area measurements (symbols) on October 13 include those of the Focused Cavity Aerosol Spectrometer (FCAS) [*Jonsson et al.*, 1995] and Multiple-Angle Aerosol Spectrometer Probe (MASP) [*Baumgardner et al.*, 1996] instruments. The line in the aerosol panel represents values estimated using the correlation with N_2O obtained on other flights in the August and October time periods.

vortex edge region on each flight leg. The location marks the latitude where the difference between the equatorward and the poleward horizontal wind gradients (after heavy smoothing) is a maximum. As shown in Figures 5 and 6, this wind-gradient reference coincides fairly consistently with sharp changes in the horizontal gradients of NO_y and O_3. Other choices of a reference location are the onset of highly enhanced ClO (> 0.15 ppbv) due to polar stratospheric cloud (PSC) processing [*Proffitt et al.*, 1989a] and the maximum in the horizontal wind [*Kawa et al.*, 1992]. Neither of these definitions yield

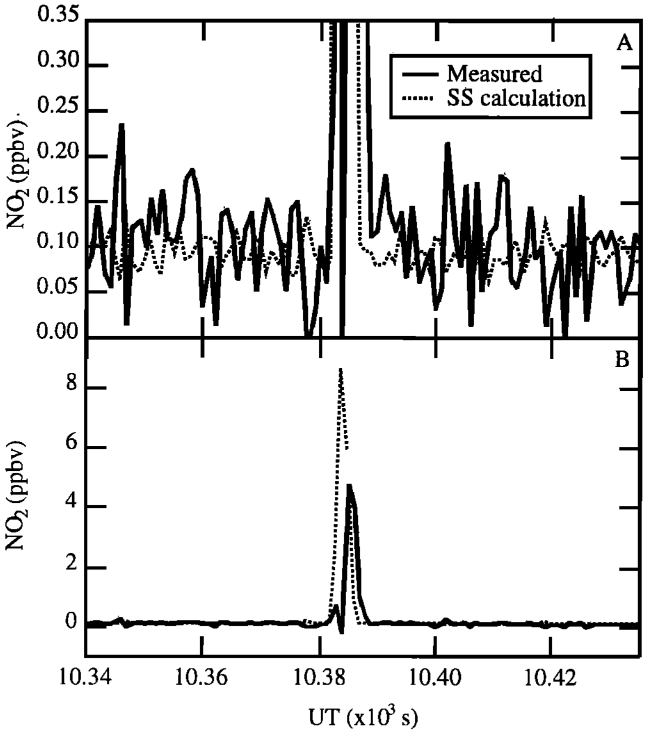

Figure 7. Segment of NO_2 measurements (1-s sample period) made on the Concorde plume sampling fight of October 8, 1994. Data are plotted as a function of UT along the ER-2 flight track. In the top panel, the vertical scale is expanded around a plume event to highlight measurements (solid line) and SS values (dashed line) (equation (8)) outside the plume. The bottom panel shows the increase in NO_2 that occurs when the Concorde plume is encountered. The time delay and change in shape noted between the measured and the SS NO_2 peaks is caused by the difference in residence time in the NO and NO_2 sample lines (see Figure 2). These differences do not affect the comparison of NO_2 values if integrated peak areas are used.

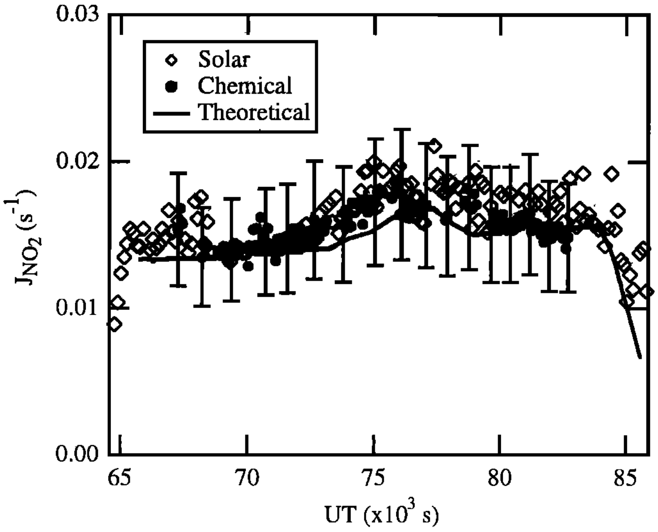

Figure 8. Values of J_{NO_2} for the flight of March 18, 1994. "Solar" values (open diamonds) are derived from solar irradiance measurements by the Composition and Photodissociative Flux Measurement instrument. "Chemical" values are derived from equation (9) using NO, NO_2, O_3, ClO, and BrO observations and averaged over 100 s (solid circles with error bars representing the total error propagated from individual measurement uncertainties). "Theoretical" values are those calculated using an atmospheric radiation-scattering model (solid line). The estimated uncertainty of the solar and theoretical values is ±15% and ±30%, respectively (see text).

consistent results for the data presented here, particularly because high ClO values are absent in nonwinter seasons (Figures 5 and 6).

Other ER-2 measurements used in the SS and PSS calculations are shown in Figures 5 and 6. Aerosol surface area measurements are not available for the first three flights due to various instrumental issues. Instead, values are estimated using the relation between aerosol and N_2O, an excellent tracer of air motion, obtained in flights preceding and following these three flights. Because the aerosol perturbations from the 1991 Mount Pinatubo eruption have decayed significantly, the aerosol surface area varies smoothly along the flight tracks. Specifically, aerosol surface areas in the lower stratosphere were in the range 1 to 5 μm^2 cm^{-3} during 1994 (*J. C. Wilson et al.*, manuscript in preparation, 1996), having decreased from peak values of 20 to 100 μm^2 cm^{-3} [*Wilson et al.*, 1993] following the Mount Pinatubo eruption.

NO and NO_2 values are both bounded by 0.3 ppbv for observations obtained in March and June 1994 (Figure 3) and by 0.3 and 0.6 ppbv, respectively, during August and October 1994 (Figure 4). For the three flights with NO_2 measurements, good agreement is found between measured and SS NO_2 values, as shown in Figures 3 and 4 and in Table 2. NO_x/NO_y values vary from 0.01 to 0.1, with the lowest values found in winter (for August 6, SS NO_2 is used to infer NO_x/NO_y in the absence of NO_2 observations). The agreement between observed abundances of NO, NO_2, and NO_x/NO_y and theoretical values found using the PSS model is also generally very good. PSS model results shown in the histogram panels of Figures 3 and 4 indicate that HNO_3 is expected to constitute more than 80% of the NO_y reservoir for the range of NO_y (2 to 11 ppbv) and O_3 (1 to 4 ppmv) sampled during the four flights. The next most abundant species are expected to be NO_x and $ClONO_2$, with other species such as N_2O_5 consistently constituting less than a few percent of the NO_y reservoir. The flight on June 1 is of special interest because the first half occurred in the dark (SZA > 92°) (Figure 3). As expected, both observed and calculated values of NO are zero since NO is converted to NO_2 in the absence of sunlight. The SS approximation (equation (8)) is not applicable in the dark because J_{NO_2} equals zero. However, the PSS model, constrained in part by measured NO_y, simulates all components of the NO_y family throughout a 24-hour period. The agreement of the PSS results for NO_2 with values observed prior to local sunrise increases confidence in our theoretical understanding of the diurnal variation of NO_y species.

As illustrated in Figure 1, NO_2 is a key species in the NO_y reservoir because it is reactively coupled to N_2O_5 which, following hydrolysis on sulfate aerosols (equation (1)), provides a reactive sink for NO_x. Furthermore, the reaction of NO_2 with oxygen atoms controls O_3 removal by NO_y species [*Wennberg et al.*, 1994]. An accurate simulation of measured NO_2 concentrations must include a realistic representation of the photolysis field and the reaction kinetics for many other species, including OH, N_2O_5, and HNO_3. Thus the ability of the PSS model to accurately simulate observed NO_2 levels for the range of conditions in Figures 3 and 4 demonstrates confidence in our understanding of the effect of heterogeneous reactions on NO_y partitioning and the impact of NO_y gases on O_3 removal rates, and in the calculated concentrations of a wide range of other species.

On the August 6 flight, NO values approached zero inside the vortex edge region, poleward of 65°S (Figure 4). Although no NO_2 observations are available for this flight, SS NO_2 values are also low. High ClO mixing ratios found in this region (Figure 6) indicate that NO_x values must be low because of enhanced $ClONO_2$ formation. In this region, PSS values for NO and NO_2 are significantly larger than observed NO and SS NO_2 values, respectively. The associated air parcels, although at temperatures above those required for PSC formation, probably underwent recent processing by PSCs that led to enhanced ClO concentrations. Back trajectory calculations show that some of the air parcels reached temperatures as low as 192 K (Figure 9) in the preceding 10 days. For these air parcels the photochemical steady state assumption is not valid, because high concentrations of ClO decay over a period of days to weeks after exposure to PSCs. The decay is controlled through the formation of NO_2 from HNO_3 photolysis and reaction with OH and through the reaction of NO_2 with ClO to reform $ClONO_2$. Thus the balance among NO_x, $ClONO_2$, and HNO_3 cannot be simulated accurately for these air parcels unless heterogeneous processing by PSCs is estimated using a separate model that includes the recent temperature and latitude history of air parcels. *Kawa et al.* [1996] and *Jaeglé et al.* (Evolution and stoichiometry of heterogeneous processing in the Antarctic stratosphere, submitted to *Journal of Geophysical Research*, 1996) demonstrate good agreement among observations of NO_x, ClO_x, and HO_x radicals and simulations using trajectory models for air parcels that have undergone recent exposure to PSCs.

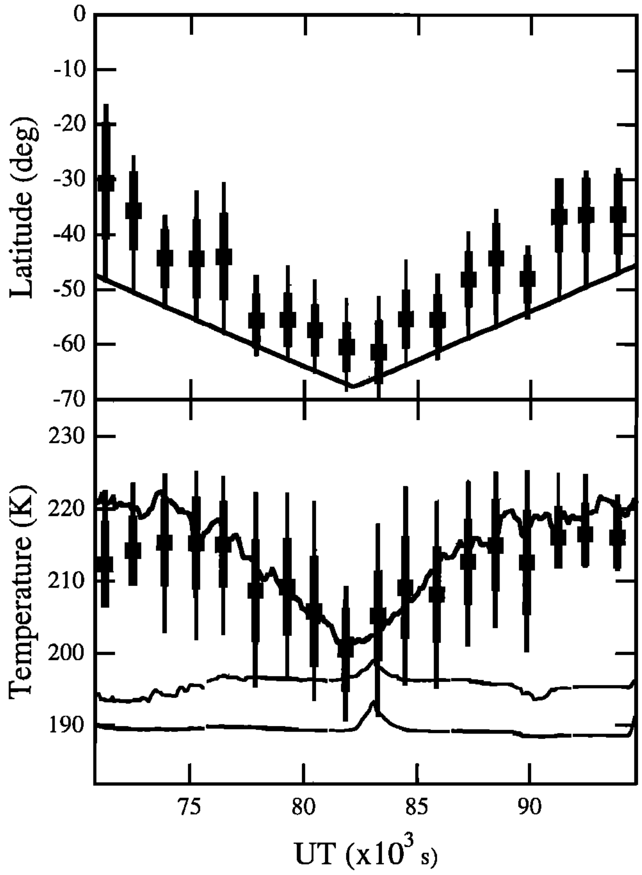

Figure 9. Results of 10-day back trajectory calculations for the flight on August 6, 1994, showing (top) latitudinal positions and (bottom) temperature. Continuous curves in each panel show flight track observations. The two lower curves in the bottom panel indicate approximate threshold temperatures for nitric acid trihydrate (upper) and ice aerosol (lower) formation. The individual points represent the mean (square), standard deviation (thick vertical line), and extrema (thin vertical line) in the trajectory values obtained during the 10 days prior to sampling at each point along the flight track.

For another portion of the 6 August flight (outbound leg, 50°S to 60°S), observed values of NO_x/NO_y and theoretical values from the PSS model differ by a factor of 2 or more, where observed NO_x is defined here as the sum of measured NO and SS NO_2. As discussed above, such differences are expected when air parcels experience recent latitude excursions of more than 15°. Indeed, 10-day back trajectory calculations indicate that these air parcels experienced latitudinal movement as large as 20° (Figure 9). In these extreme cases the PSS calculations represent a limit for observed NO_x values. When the recent movement is poleward, toward lower average insolation, PSS values for NO_2 and NO are expected to be lower than observed values. This expectation is consistent with the comparison between theory and observation outside the vortex on August 6 (Figure 4). *Kawa et al.* [1993] found that for one high-latitude case, good agreement between theory and observation for NO required using a photochemical model that accounted for the variations of latitude and temperature during the last 10 days. In general, smaller-latitude excursions of 10° or less are not expected to lead to noticeable discrepancies.

The low NO_x/NO_y levels during winter (1 June and 6 August) are the combined result of heterogeneous reactions on aerosol particle surfaces, higher O_3 concentrations, and low average insolation. The heterogeneous reactions (1) to (3) on sulfate aerosol have been demonstrated in the laboratory [*Tolbert et al.*, 1988; *Hanson and Ravishankara*, 1991; *Van Doren et al.*, 1991; *Hanson et al.*, 1996] and have been inferred from observations [*McElroy et al.*, 1992; *Keys et al.*, 1993; *Fahey et al.*, 1993; *Toon et al.*, 1993; *Koike et al.*, 1993, 1994]. The lowest measured value of the NO_x/NO_y ratio, shown in Figure 3 for 1 June, is ~0.01. The related value of NO_x is near the detection limit of the chemiluminescence detectors. These direct measurements confirm previous studies that inferred the presence of low NO_x/NO_y values in the winter polar vortices [*Fahey et al.*, 1990; *Kawa et al.*, 1993]. As an illustration of the effect that heterogeneous processes have on partitioning the NO_y reservoir, heterogeneous reaction rates were set to zero in the PSS model. The results, expressed as the ratio of NO_x calculated using only gas phase chemistry to that using both heterogeneous and gas phase chemistry, are shown in Figure 10 for 1 June. The large values of this ratio demonstrate the importance of heterogeneous chemistry for regulating NO_y partitioning in the winter polar regions.

The latitudinal and seasonal dependence of the NO_x/NO_y and $ClONO_2/NO_y$ ratios calculated using the PSS model are shown in Figure 11. Only the return legs to Christchurch are shown

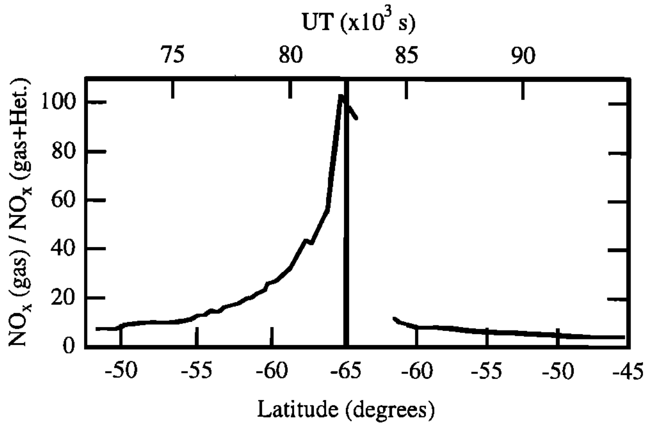

Figure 10. Ratio of NO_x calculated using gas phase chemistry to that using both heterogeneous and gas phase chemistry from the PSS model results for the flight of June 1, 1994 for pressures between 53 and 73 mbar.

because the ambient pressure ranges were similar for each of the four flights (Figures 5 and 6). NO_x/NO_y values, as discussed above, are reduced dramatically during winter, especially at the highest latitudes. However, in October (spring) the NO_x/NO_y ratio returns to similar values found for March (fall) values. The $ClONO_2/NO_y$ ratio shows opposite changes with season, with larger values occurring in winter. However, values are still much higher for October than for March. The $ClONO_2/NO_y$ ratio shows more flight-to-flight variability than the NO_x/NO_y ratio, as well as more variability within individual flights. The increased variability originates from the fact that model values for $ClONO_2/NO_y$ are constrained not only by measured NO_y but also by total Cl_y as observed from concentrations of chlorinated source gases. As illustrated in Figure 12, Cl_y for the return legs of the four flights, as derived from N_2O using the relation of *Woodbridge et al.* [1995], varied significantly within individual flights and from flight to flight.

Conclusions

In situ measurements of NO, NO_2, and NO_y have been obtained in the lower stratosphere of the southern hemisphere at midlatitudes and inside and near the edge of the Antarctic vortex. The measurements were made over multiweek periods in the fall, winter, and spring seasons as part of the 1994 ASHOE/MAESA campaign. NO_2 mixing ratio values were calculated using a steady state approximation (equation (8)) that incorporates simultaneous observations of NO, O_3, ClO, and BrO, and J_{NO2} values calculated using a radiative transfer model. These calculated NO_2 values agree well with measured NO_2 values throughout the data set, except inside the Concorde exhaust plume where measured NO_2 values were significantly lower. Averaged over the 10 flights for which NO_2 observations are available, measured mixing ratios of

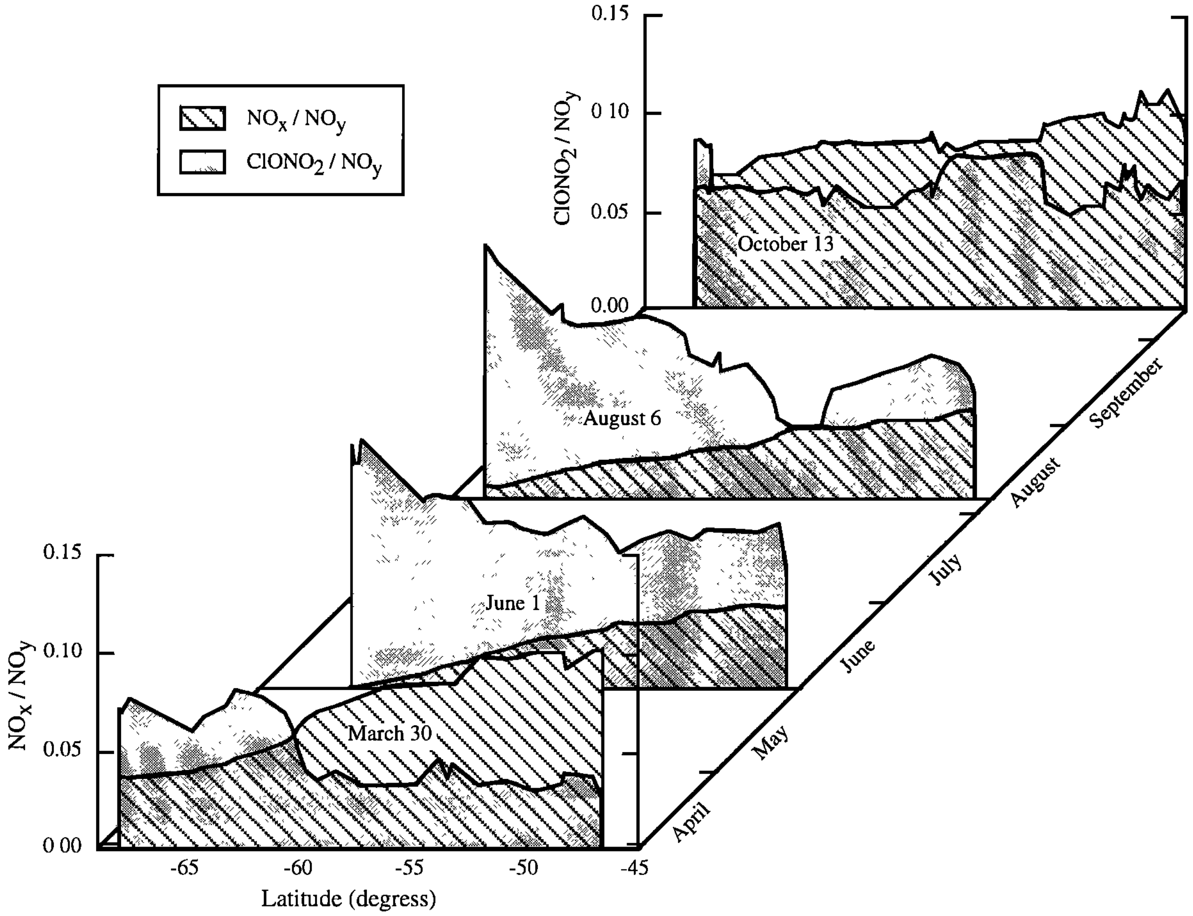

Figure 11. NO_x/NO_y (striped) and $ClONO_2/NO_y$ (shaded) ratios from PSS model calculations shown as a function of time and latitude for the flights in Figures 3 and 4.

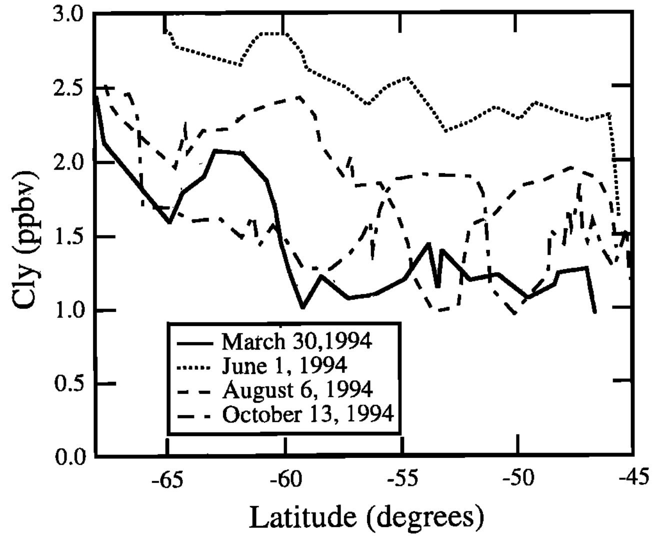

Figure 12. Cl_y used in the PSS model calculations for the flights shown in Figures 3 and 4.

NO_2 are ~8% lower than calculated values. This difference is significantly smaller than the uncertainty of the measurements, and much less than the differences found in a similar comparison using data acquired during the SPADE campaign. On the basis of the comparisons presented here, we do not recommend any corrections to J_{NO_2} values calculated from the radiation scattering models or to the rate constants used in the steady state calculations.

Excellent agreement was found for NO_2 photolysis rates estimated three ways: derived from direct measurements of solar flux, inferred from measured concentrations of reactive species, and calculated using a radiative transfer model. The "solar" photolysis rate relies on in situ observations of the solar flux in the UV region and laboratory photodissociation cross sections for NO_2. The "chemical" rate is found using a steady state relation that incorporates in situ observations of concentrations of NO, NO_2, O_3, ClO, and BrO and laboratory reaction rate coefficients. The "theoretical" rate is obtained using a radiation scattering model with full spherical symmetry and multiple-scattering processes, constrained by satellite observations of total O_3 and UV reflectivity. The agreement of the "solar," "chemical," and "theoretical" rates of NO_2 photolysis indicates a strong self-consistency in our understanding of the transmission of UV radiation in the lower stratosphere, the influence of UV radiation on reactive species, and the kinetics of processes that partition NO and NO_2.

A full diurnal photochemical model simulation was also used for comparison to the NO and NO_2 observations. In general, the agreement between observation and theory for the NO_x/NO_y ratio is excellent, with exceptions attributed to the absence of steady state conditions caused by recent PSC processing or large and rapid latitude excursions. Our observations show that the NO_x/NO_y ratio is reduced significantly at high latitudes during winter and subsequently recovers in the spring, consistent with the previous in situ observations of NO and NO_y [*Fahey et al.*, 1990; *Kawa et al.*, 1993]. As a result of the low observed NO_x/NO_y ratios, HNO_3 is expected to comprise 80% or more of the NO_y reservoir throughout mid to high latitudes in the lower stratosphere. The agreement of observation and theory for NO_x/NO_y demonstrates that heterogeneous processes of sulfate aerosols regulate the partitioning of the NO_y reservoir for a wide range of lower stratospheric conditions. Our results suggest that photochemical models properly constrained by observations and incorporating the latest kinetic values for gas phase and heterogeneous reaction rates as well as absorption cross sections are well suited to represent the partitioning within the NO_y reservoir and the coupling to other reactive species.

Acknowledgments. This work was supported by the NASA High Speed Research Program and the Upper Atmosphere Research Program.

References

Anderson, D. E., R. DeMajistre, S. A. Lloyd, and P. K. Swaminathan, Photodissociation in the troposphere and stratosphere: Radiation field models for clouds, aerosols, and twilight, *J. Geophys. Res.*, *100*, 7135-7145, 1995.

Baumgardner, D., J. E. Dye, B. Gandrud, K. Barr, K. K. Kelly, and K. R. Chan, Refractive indices of aerosols in the upper troposphere and lower stratosphere, *Geophys. Res. Lett.*, *23*, 749-752, 1996.

Bevington, P. R., *Data Reduction and Error Analysis for the Physical Sciences*, McGraw-Hill, New York, 1969.

Brune, W. H., J. G. Anderson, and K. R. Chan, In situ observations of BrO over Antarctica: ER-2 aircraft results from 54°S to 72°S latitude, *J. Geophys. Res.*, *94*, 16,639-16,647, 1989a.

Brune, W. H., J. G. Anderson, and K. R. Chan, In situ observations of ClO over Antarctica: ER-2 aircraft results from 54°S to 72°S latitude, *J. Geophys. Res.*, *94*, 16,649-16,663, 1989b.

Carroll, M. A., D. D. Montzka, G. Hübler, and K. K. Kelly, In situ measurements of NO_x in the Airborne Arctic Stratospheric Expedition, *Geophys. Res. Lett.*, *17*, 493-496, 1990.

Cohen, R. C., et al., Are models of catalytic removal of O_3 by HO_x accurate? Constraints from in situ measurements of the OH to HO_2 ratio, *Geophys. Res. Lett.*, *21*, 2539-2542, 1994.

DeMore, W. B., S. P. Sander, D. M. Golden, R. F. Hampson, M. J. Kurylo, C. J. Howard, A. R. Ravishankara, C. E. Kolb, and M. J Molina, Chemical kinetics and photochemical data for use in stratospheric modeling, *JPL Publ., 94-26,* Jet Propul. Lab., Pasadena, Calif., 1994.

Fahey, D. W., K. K. Kelly, G. V. Ferry, L. R. Poole, J. C. Wilson, D. M. Murphy, M. Loewenstein, and K. R. Chan, In situ measurements of total reactive nitrogen, total water, and aerosol in a polar stratospheric cloud in the Antarctic, *J. Geophys. Res.*, *94*, 11,299-11,315, 1989.

Fahey, D. W., S. R. Kawa, and K. R. Chan, Nitric oxide measurements in the Arctic winter stratosphere, *Geophys. Res. Lett.*, *17*, 489-492, 1990.

Fahey, D. W., et al., In situ measurements constraining the role of sulphate aerosols in mid-latitude ozone depletion, *Nature*, *363*, 509-514, 1993.

Fahey, D. W., et al., Emission measurements of the Concorde supersonic aircraft in the lower stratosphere, *Science*, *270*, 70-74, 1995a.

Fahey, D. W., et al., In situ observations in aircraft exhaust plumes in the lower stratosphere at midlatitudes, *J Geophys. Res.*, *100*, 3065-3074, 1995b

Folkins, I., A. J. Weinheimer, G. Brasseur, F. LeFèvre , B. A. Ridley, J. G. Walega, J. E. Collins, and R. F. Pueschel, Three-dimensional model interpretation of NO_x measurements from the lower stratosphere, *J. Geophys. Res.*, *99*, 23,117-23,129, 1994.

Gao, R. S., E. R. Keim, E. L. Woodbridge, S. J. Ciciora, M. H. Proffitt, T. L. Thompson, R. J. McLaughlin, and D. W. Fahey, New photolysis system for NO_2 measurements in the lower stratosphere, *J. Geophys. Res.*, *99*, 20,673-20,681, 1994.

Hanson, D. R., and A. R. Ravishankara, The reaction probabilities of $ClONO_2$ and N_2O_5 on 40 to 75 percent sulfuric acid solutions, *J. Geophys. Res* , *96*, 17,307-17,314, 1991.

Hanson, D. R., and A. R. Ravishankara, Reactive uptake of $ClONO_2$ onto sulfuric acid due to reaction with HCl and H_2O, *J. Phys. Chem*, *98*, 5728-5735, 1994.

Hanson, D. R., A. R. Ravishankara, and S. Solomon, Heterogeneous reactions in sulfuric acid aerosols: A framework for model calculations, *J. Geophys. Res.*, *99*, 3615-3629, 1994.

Hanson, D. R., and A. R. Ravishankara, Heterogeneous chemistry of bromine species in sulfuric acid under stratospheric conditions, *Geophys. Res. Lett.*, *22*, 385-388, 1995.

Hanson, D. R., A. R. Ravishankara, and E. R. Lovejoy, Reaction of BrONO2 with H_2O on submicron sulfuric acid aerosol and the implications for the lower stratosphere, *J. Geophys. Res.*, *101*, 9063-9069, 1996.

Hastie, D. R., and M. D. Miller, Balloon-borne tunable diode laser absorption spectrometer for multispecies trace gas measurements in the stratosphere., *Appl. Opt.*, *24*, 3694-3701, 1985.

Helten, M., W. Patz, M. Trainer, H. Fark, E. Klein, and D. H. Ehhalt, Measurements of stratospheric HO_2 and NO_2 by matrix isolation and ESR spectroscopy, *J. Atmos. Chem.*, *2*, 191-202, 1984.

Helten, M., W. Patz, D. H. Ehhalt, and E. P. Roeth, Measurements of nighttime NO_3 and NO_2 in the stratosphere by matrix isolation and ESR spectroscopy, in *Atmospheric Ozone*, edited by C. S. Zerefos and A. Ghazi, pp. 196-200, D. Reidel, Norwell, Mass., 1985.

Jaeglé, L., et al., In situ measurements of the NO_2/NO ratio for testing atmospheric photochemical models, *Geophys. Res. Lett.*, *21*, 2555-2558, 1994.

Jonsson, H. H., et al., Performance of a focused cavity aerosol spectrometer for measurements in the stratosphere of particle size in the 0.06-2.0 μm diameter range, *J. Atmos. Oceanic Tech.*, *12*, 115-129, 1995.

Kawa, S. R., D. W. Fahey, S. Solomon, W. H. Brune, M. H. Proffitt, D. W. Toohey, D. E. Anderson Jr., L. C. Anderson, and K. R. Chan, Interpretation of aircraft measurements of NO, ClO, and O_3 in the lower stratosphere, *J. Geophys. Res.*, *95*, 18,597-18,609, 1990.

Kawa, S. R., et al., Photochemical partitioning of the reactive nitrogen and chlorine reservoirs in the high-latitude stratosphere, *J. Geophys. Res.*, *97*, 7905-7923, 1992.

Kawa, S. R., et al., Interpretation of NO_x/NO_y observations from AASE-II using a model of chemistry along trajectories, *Geophys. Res. Lett.*, *20*, 2507-2510, 1993.

Kawa, S. R., et al., Activation of chlorine in sulfate aerosol as inferred from aircraft observations, *J. Geophys. Res.*, this issue.

Keys, J. G., P. V. Johnston, R. D. Blatherwick, and F. J. Murcray, Evidence for heterogeneous reactions in the Antarctic autumn stratosphere, *Nature*, *361*, 49-51, 1993.

Koike, M., Y. Kondo, W. A. Matthews, P. V. Johnston, and K. Yamazaki, Decrease of stratospheric NO_2 at 44°N caused by Pinatubo volcanic aerosols, *Geophys. Res. Lett.*, *20*, 1975-1978, 1993.

Koike, M., N. B. Jones, W. A. Matthews, P. V. Johnston, R. L. McKenzie, D. Kinnison, and J. Rodriguez, Impact of Pinatubo aerosols on the partitioning between NO_2 and HNO_3, *Geophys. Res. Lett.*, *21*, 597-600, 1994.

Kolb, C. E., et al., Laboratory studies of atmospheric heterogeneous chemistry, in *Progress and Problems in Atmospheric Chemistry*, Edited by J. R. Barker, World Scientific Publishing, Singapore, 1995.

Kondo, Y., P. Aimedieu, M. Koike, Y. Iwasaka, P A. Newman, U. Schmidt, W. A. Matthews, M. Hayashi, and W. R. Sheldon, Reactive nitrogen, ozone, and nitrate aerosols observed in the Arctic stratosphere in January 1990, *J. Geophys. Res.*, *97*, 13,025-13,038, 1992.

Logan, J. A., M. J. Prather, S. C. Wofsy, and M. B. McElroy, Atmospheric chemistry: Response to human influence, *Philos. Trans. R. Soc. BA*, *290*, 187-234, 1978.

McElroy, C. T., A spectroradiometer for the measurement of direct and scattered solar irradiance from on-board the NASA ER-2 high-altitude research aircraft, *Geophys. Res. Lett.*, *22*, 1361-1364, 1995.

McElroy, C. T., C. Midwinter, D. V. Barton, and R. B. Hall, A comparison of J-values from the composition and photodissociative flux measurement with model calculations, *Geophys. Res. Lett.*, *22*, 1365-1368, 1995.

McElroy, M. B., R. J. Salawitch, S. C. Wofsy, and J. A. Logan, Reduction of Antarctic ozone due to synergistic interactions of chlorine and bromine, *Nature*, *321*, 759-762, 1986.

McElroy, M. B., R. J. Salawitch, and K. Minschwaner, The changing stratosphere, *Planet. Space Sci.*, *40*, 373-401, 1992.

McFarland, M., B. A. Ridley, M. H. Proffitt, D. L. Albritton, T. L. Thompson, W. J. Harrop, R. H. Winkler, and A. L. Schmeltekopf, Simultaneous in situ measurements of nitrogen dioxide, nitric oxide, and ozone between 20 and 31 km, *J. Geophys. Res.*, *91*, 5421-5437, 1986.

Michelsen, H. A., R. J. Salawitch, P. O. Wennberg, and J. G. Anderson, Production of $O(^1D)$ from photolysis of O_3, *Geophys. Res. Lett.*, *21*, 2227-2230, 1994.

Prather, M. J., Ozone in the upper stratosphere and mesosphere, *J. Geophys. Res.*, *86*, 5325-5338, 1981.

Proffitt, M. H., et al., A chemical definition of the boundary of the Antarctic ozone hole, *J. Geophys. Res.*, *94*, 11,437-11,448, 1989a.

Proffitt, M. H., et al., In situ ozone measurements within the 1987 Antarctic ozone hole from a high-altitude ER-2 aircraft, *J. Geophys. Res.*, *94*, 16,547-16,556, 1989b.

Ridley, B. A., M. A. Carroll, G. L. Gregory, and G. W. Sachse, NO and NO_2 in the troposphere: Technique and measurements in regions of a folded tropopause, *J. Geophys. Res.*, *93*, 15,813-15,830, 1988.

Rodriguez, J. M., M. K. W. Ko, and N. D. Sze, Role of heterogeneous conversion of N_2O_5 on sulphate aerosols in global ozone losses, *Nature*, *352*, 134-137, 1991.

Salawitch, R. J., et al., The distribution of hydrogen, nitrogen, and chlorine radicals in the lower stratosphere: Implications for changes in O_3 due to emission of NO_y from supersonic aircraft, *Geophys. Res. Lett.*, *21*, 2547-2550, 1994a.

Salawitch, R. J., et al., The diurnal variation of hydrogen, nitrogen, and chlorine radicals: Implications for the heterogeneous production of HNO_2, *Geophys. Res. Lett.*, *21*, 2551-2554, 1994b.

Schauffler, S. M., L. E. Heidt, W. H. Pollock, T. M. Gilpin, J. F. Vedder, S. Solomon, R. A. Lueb, and E. L. Atlas, Measurements of halogenated organic compounds near the tropical tropopause, *Geophys. Res. Lett.*, *20*, 2567-2570, 1993.

Scott S. G., T. P. Bui, K. R. Chan, and S. W. Bowen, The meteorological measurement system on the NASA ER-2 aircraft, *J. Atmos. Oceanic Tech.*, *7*, 525-540, 1990.

Solomon, S., R. R. Garcia, F. S. Rowland, and D. J. Wuebbles, On the depletion of Antarctic ozone, *Nature*, *321*, 755-758, 1986.

Stimpfle, R. M., et al., The response of ClO radical concentrations to variations in NO_2 radical concentrations in the lower stratosphere, *Geophys. Res. Lett.*, *21*, 2543-2546, 1994.

Stolarski, R. S., et al., 1995 Scientific assessment of the atmospheric effects of stratospheric aircraft, *NASA Ref. Publ. 1381*, Washington, D. C., 1995.

Tolbert, M. A., M. J. Rossi, and D. M. Golden, Heterogeneous interactions of $ClONO_2$, HCl, and HNO_3 with sulfuric acid surfaces at stratospheric temperature, *Geophys. Res. Lett.*, *15*, 851-854, 1988.

Toon, O., et al., Heterogeneous reaction probabilities, solubilities, and the physical state of cold volcanic aerosols, *Science*, *261*, 1136-1140, 1993.

Van Doren, J. M., L. R. Watson, P. Davidovits, D. R. Worsnop, M. S. Zahniser, and C. E. Kolb, Uptake of N_2O_5 and HNO_3 by aqueous sulfuric acid droplets, *J. Phys. Chem.*, *95*, 1684-1689, 1991.

Webster, C. R., NO_2/NO partitioning as a test of stratospheric ClO concentrations over Antarctica, *Geophys. Res. Lett.*, *14*, 704-706, 1987.

Wennberg, P. O., et al., Removal of stratospheric O_3 by radicals: In situ measurements of OH, HO_2, HO, NO_2, ClO, and BrO, *Science*, *266*, 398-404, 1994.

Wennberg, P. O., T. F. Hanisco, R. C. Cohen, R. M. Stimpfle, L. B. Lapson, and J. G. Anderson, In situ measurements of OH and HO_2 in the upper troposphere and stratosphere, *J. Atmos. Sci.*, *52*, 3413-3420, 1995.

Wilson, J. C., et al., In situ observations of aerosol and chlorine monoxide after the 1991 eruption of Mount Pinatubo: Effects of reactions on sulfate aerosol, *Science*, *261*, 1140-1143, 1993.

Woodbridge, E. L., et al., Estimates of total organic and inorganic chlorine in the lower stratosphere from in situ and flask measurements during AASE II, *J. Geophys. Res.*, *100*, 3057-3064, 1995.

L. A. Del Negro, S. G. Donnelly, D. W. Fahey, R. S. Gao, (corresponding author), E. R. Keim, M. H. Proffitt, and R. C. Wamsley, 325 Broadway, R/E/AL6, Aeronomy Laboratory, National Oceanic and Atmospheric Administration, Boulder, CO 80303..

R. J. Salawitch, Jet Propulsion Laboratory, Pasadena, CA 91109.

D. E. Anderson, R. Demajistre, and S. A. Lloyd, Applied Physics Laboratory, Johns Hopkins University, Laurel, MD 20723-6099.

C. T. McElroy, Atmospheric Environment Service/Canada, Downsview, Ontario, Canada M3H 5T4.

E. L. Woodbridge, Scripps Institution of Oceanography, University of California at San Diego, La Jolla, CA 92093.

R. M. Stimpfle and D. W. Kohn, Department of Chemistry, Harvard University, Cambridge, MA 02138.

S. R. Kawa and L. R. Lait, NASA Goddard Space Flight Center, Greenbelt, MD 20771.

K. R. Chan, M. Loewenstein, and J. R. Podolske, NASA Ames Research Center, Moffett Field, CA 94035.

J. E. Dye, Mesoscale and Microscale Meteorology Division, National Center for Atmospheric Research, Boulder, CO 80307.

J. C. Wilson, Department of Engineering, University of Denver, Denver, CO 80208.

(Received October 4, 1995; revised June 18, 1996;
accepted June 18, 1996.)